Article

# Photo- and Metal-Mediated Deconstructive Approaches to Cyclic Aliphatic Amine Diversification

David M. Soro,[#] Jose B. Roque,[#] Jonas W. Rackl, Bohyun Park, Stefan Payer, Yuan Shi, J. Craig Ruble, Alexey L. Kaledin, Mu-Hyun Baik,* Djamaladdin G. Musaev,* and Richmond Sarpong*

ACCESS | Metrics & More | Article Recommendations | Supporting Information

**ABSTRACT:** Described herein are studies toward the core modification of cyclic aliphatic amines using either a riboflavin/photo-irradiation approach or Cu(I) and Ag(I) to mediate the process. Structural remodeling of cyclic amines is explored through oxidative C−N and C−C bond cleavage using peroxydisulfate (persulfate) as an oxidant. Ring-opening reactions to access linear aldehydes or carboxylic acids with flavin-derived photocatalysis or Cu salts, respectively, are demonstrated. A complementary ring-opening process mediated by Ag(I) facilitates decarboxylative Csp³−Csp² coupling in Minisci-type reactions through a key alkyl radical intermediate. Heterocycle interconversion is demonstrated through the transformation of N-acyl cyclic amines to oxazines using Cu(II) oxidation of the alkyl radical. These transformations



are investigated by computation to inform the proposed mechanistic pathways. Computational studies indicate that persulfate mediates oxidation of cyclic amines with concomitant reduction of riboflavin. Persulfate is subsequently reduced by formal hydride transfer from the reduced riboflavin catalyst. Oxidation of the cyclic aliphatic amines with a Cu(I) salt is proposed to be initiated by homolysis of the peroxy bond of persulfate followed by α-HAT from the cyclic amine and radical recombination to form an α-sulfate adduct, which is hydrolyzed to the hemiaminal. Investigation of the pathway to form oxazines indicates a kinetic preference for cyclization over more typical elimination pathways to form olefins through Cu(II) oxidation of alkyl radicals.
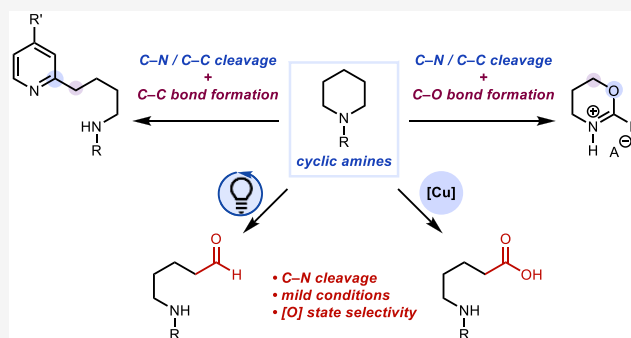
## INTRODUCTION

Modern drug discovery has benefited from advancements in chemical reaction development.[1] For example, the development of selective C−H functionalization has changed how synthetic chemists approach the retrosynthetic analysis of bioactive compounds.[2] Largely, disconnections of molecules to simpler precursors through a retrosynthesis exercise focus on removal of peripheral groups.[3,4] As a result, in the forward sense, syntheses and late-stage diversification of molecules have mostly focused on peripheral modification. Alternatively, an emerging approach to access novel chemical space has been centered around making modifications to the core framework of molecules, contrasting traditional molecular structural diversification approaches.[5,6] Recognizing a need for more methods to accomplish modification of the core framework of molecules (skeletal editing) to access unique chemical and functional space, we have initiated a program aimed at the deconstructive functionalization (i.e., breaking of traditionally strong bonds, such as C−C and C−N bonds, and functionalization of their constituent atoms) of saturated cyclic amines in order to access new chemical space. We have primarily focused on saturated azacycles, especially piperidines, given their prevalence in pharmaceuticals,[7] as well as

agrochemicals.[8] Our previous studies have identified ring opening,[9] ring contraction,[10] as well as heterocycle replacement remodeling methods[11] for achieving skeletal diversity (Figure 1A).

We have found oxidative pathways to be particularly effective for the deconstructive functionalization of cyclic aliphatic amines (saturated azacycles).[9,10] In complementary approaches, others have demonstrated oxidative bond cleavage of cyclic amines under aerobic conditions[12−14] as well as through the use of metal-oxo species.[15−17] While these strategies provide effective ways to achieve diversity in cyclic amine transformations, metal-oxo catalysts tend to favor oxidative pathways leading to imide products;[18] peripheral modification is favored over core modification for these catalysts. Our goal was to develop a straightforward, distinct approach that would achieve a reconfiguration of the cyclic
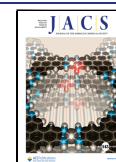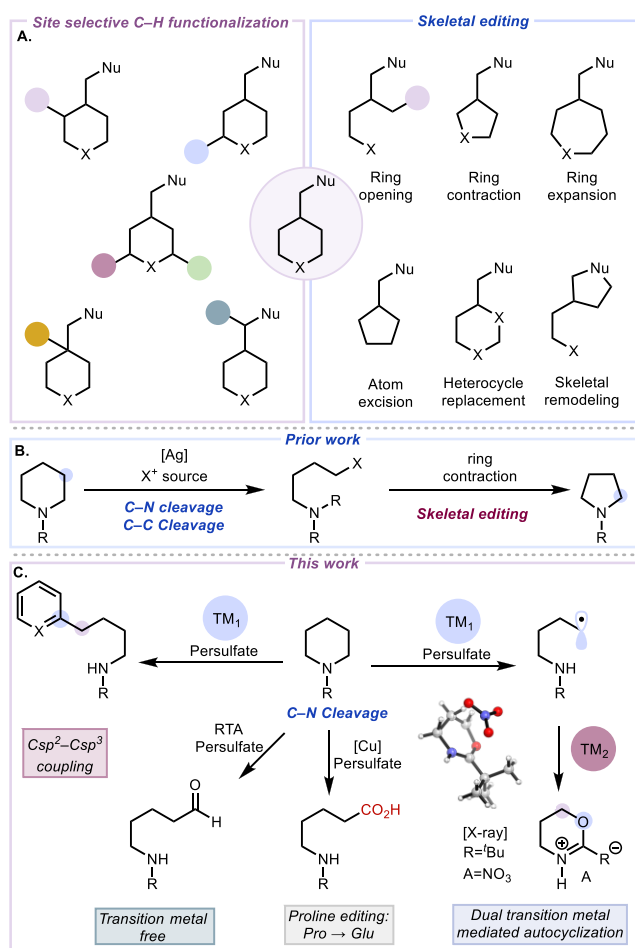
**Figure 1.** (A) Skeletal editing. (B) Prior work. (C) This work.

amine skeleton through structural transformations beyond ring opening. Peroxydisulfate (persulfate) has been shown to be a versatile oxidant in various contexts. Given its high oxidation potential (redox potential = 2.01 V in aqueous solution),[19,20] the redox reactivity of persulfate with transition metals or organic substrates can lead to different outcomes. In particular, persulfate has been used in the oxidative functionalization of amines, providing access to $\alpha$-amino radicals and iminium intermediates.[21] On this basis, our lab previously reported the deconstructive diversification of cyclic amines using a Ag(I)-persulfate combination (Figure 1B).[9,10] With the goal of increasing the diversity of scaffolds that could be accessed, we envisioned that persulfate might serve a key role in the deconstructive functionalization of saturated cyclic amines by mediating the cleavage of the C−N bond to provide novel acyclic structures. By pairing the persulfate oxidant with various redox-active co-reagents, we anticipated tuning the deconstructive process in order to access a broad range of scaffolds.

Herein, we present complementary efforts that achieve saturated azacycle diversification. Specifically, we report (i) two mild oxidative ring-opening methods using riboflavin-persulfate and copper-persulfate combinations that generate aldehydes and acyclic alkyl carboxylic acids, respectively, (ii) direct $Csp^2$−$Csp^3$ bond formation through a ring-opening/Minisci process, and (iii) autocyclization by leveraging a dual transition metal system to convert between heterocycles (Figure 1C).

Flavins, a set of molecules featuring an isoalloxazine core (Figure 2A), are key facilitators in a subset of biological electron transfer processes including the oxidation of amines by monoamine oxidases.[22] They have also been used in nonbiological contexts for similar purposes.[23] As such, we wondered whether they could effect nonbiological oxidative diversification of cyclic aliphatic amines. A general mechanism for our proposed transformation of saturated cyclic amines using the riboflavin-persulfate system is depicted in Figure 2B. Excitation of an isoalloxazine derivative (**2.A**) was expected to generate an excited state photocatalyst (**2.B\***). This excited state species should then oxidize cyclic amine **1a** via photoinduced electron transfer to produce an amidyl radical cation (**1a$_{ox}$**) and reduced photocatalyst (**2.C**). Oxidation of the reduced photocatalyst by a persulfate ion would regenerate quinone **2.A** as well as a sulfate radical anion. The sulfate radical anion was anticipated to effect $\alpha$-amino C−H abstraction of **1a$_{ox}$** to generate iminium ion **1.A**. As previously proposed by us using the combination of Ag(I) and persulfate,[9,10] the resulting iminium ion (**1.A**) would then be trapped by $H_2O$ to give hemiaminal **1.B**, which would suffer heterolytic C−N bond cleavage to furnish aldehyde **3a**. A pivaloyl group on the nitrogen atom was identified previously to be optimal in favoring the open-chain aminoaldehyde product (**3a**).[10]

## ■ RESULTS AND DISCUSSION

**Bio-Inspired Deconstructive Functionalization.** We commenced our investigations of the oxidative C−N bond cleavage by evaluating a broad range of photoredox catalysts, oxidants, and solvent combinations (see the Supporting Information for details). After extensive optimization, we identified the conditions shown in Figure 2C that employ 5 mol % of riboflavin tetraacetate (**2a**), 3 equivalents of $K_2S_2O_8$ in a 1:1 (v/v) mixture of MeCN/$H_2O$, and irradiation with blue light-emitting diodes (Kessil brand A160WE Tuna Blue LED 40 W lamp).

We considered whether the riboflavin photocatalyst might operate through the fully oxidized quinone state (see **2.A** in Figure 2D) as well as the one-electron-reduced semiquinone state (see **2.E** in Figure 2D) without reaching the fully reduced hydroquinone state (see **2.F** in Figure 2D) although that remained to be fully supported by additional studies. We hypothesized that upon generation of semiquinone **2.E**, oxidation by persulfate occurs to regenerate **2.A**, the corresponding sulfate dianion, and sulfate radical anion. Furthermore, the sulfate radical anion can also oxidize semiquinone **2.E**. Performing the reaction without sparging the reaction mixture (entry 1) led to a slightly diminished yield, presumably due to some catalyst deactivation by molecular oxygen. In the absence of riboflavin tetraacetate, only a 30% yield of product is obtained (entry 2). Likely, in this case, the product arises from light or thermal activation in which the homolytic O−O cleavage of the persulfate leads to two sulfate radical anions, which effect $\alpha$-amino C−H abstraction followed by single-electron oxidation to generate **1.A** (Scheme 1). An alternative productive pathway, given the oxidizing strength of sulfate radical anions [+2.4 V vs saturated calomel electrode (SCE)], could proceed through an initial oxidation of the substrate prior to $\alpha$-amino C−H abstraction.[24] The light-driven homolysis of persulfate has been previously reported.[20] Unfortunately, increased loadings of $K_2S_2O_8$ along with increased temperature, and/or longer reaction times did
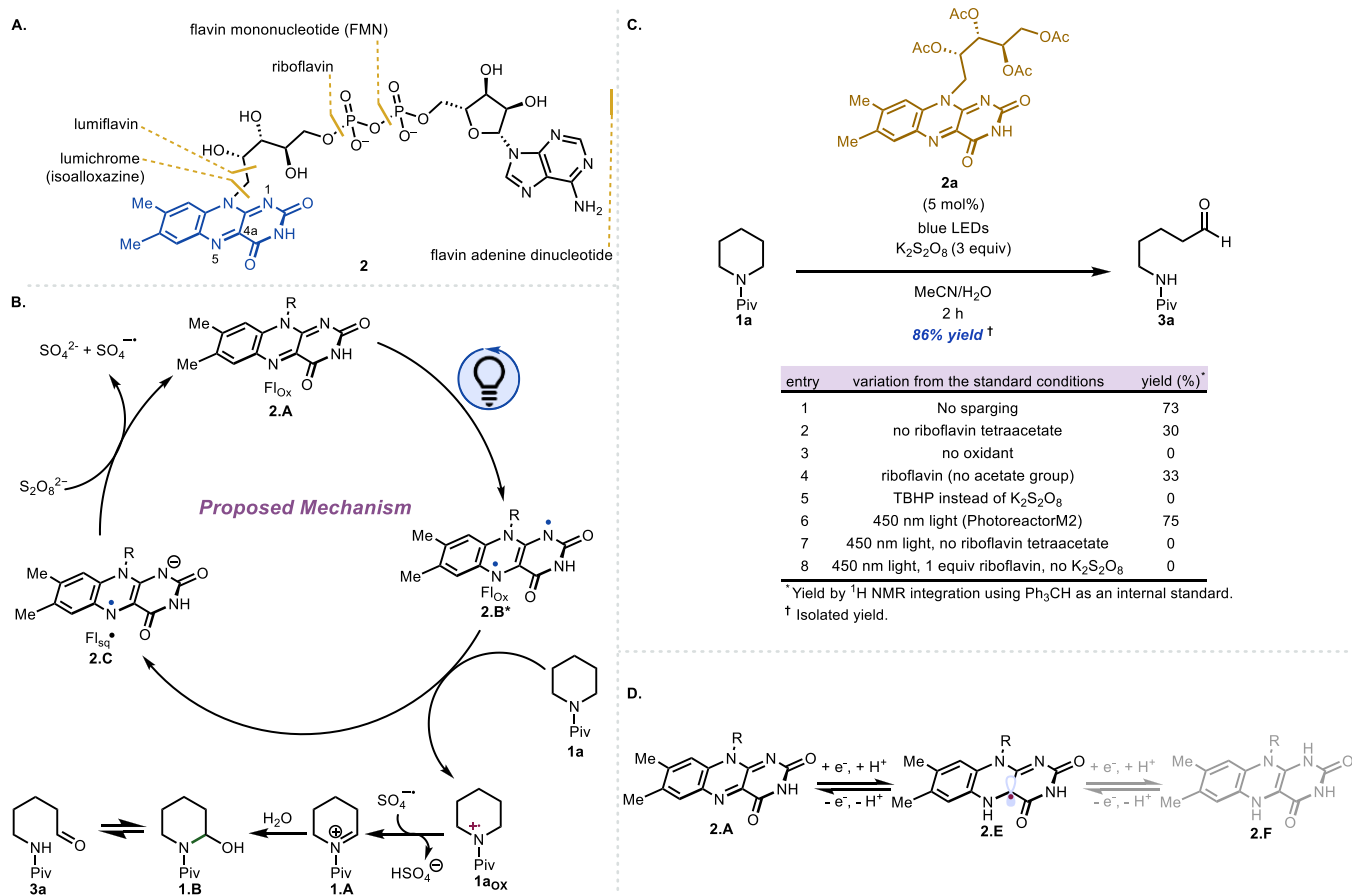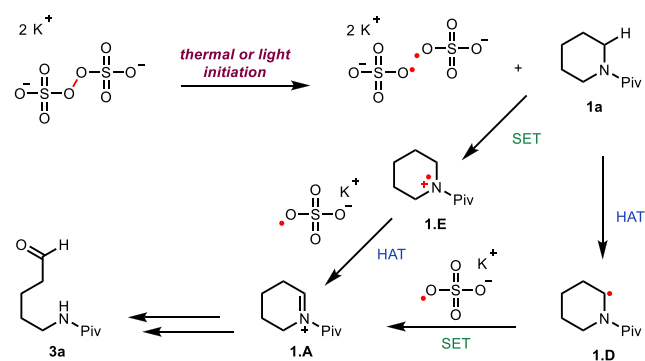
**Figure 2.** (A) Flavin derivatives. (B) Proposed reaction mechanism for the ring-opening oxidation of cyclic amines using riboflavin tetraacetate. (C) Selected reaction optimization experiments (see the Supporting Information for full details). (D) Typical redox states of flavin molecules.

## Scheme 1. Light- or Thermal-Driven Homolysis of Persulfate



not improve the yield, leading instead to undesired reactivity such as over-oxidation. The use of riboflavin instead of riboflavin tetraacetate also led to diminished yields (entry 4). Riboflavin has been reported to undergo rapid photo-degradation upon irradiation,[25,26] which might contribute to the decreased yields. The acetylation of the ribose side chain (i.e., riboflavin → riboflavin tetraacetate) presumably prevents competing intramolecular hydrogen atom transfer (HAT) from the $T_1$ excited state.[27]

In our studies, persulfate emerged as the superior oxidant as other oxidants led to lower yields (entry 5). Control studies confirmed the importance of both the oxidant and light source as the desired product was not observed when either

component was excluded from the reaction mixture. Irradiation with 450 nm blue light-emitting diodes (LEDs, Penn PhD Photoreactor M2) in the absence of riboflavin tetraacetate led to recovered starting material (entry 7). Presumably, O−O bond homolysis does not occur with irradiation at 450 nm,[28] which is also supported by our calculated UV−Vis spectrum of $K_2S_2O_8$ (see the Supporting Information). Additionally, the use of one equivalent of riboflavin tetraacetate as the sole oxidant in the reaction led only to recovery of the starting material without any observed product formation. However, upon the combination of 5 mol % of riboflavin tetraacetate with persulfate, a 75% yield of aldehyde **3a** was obtained (entry 6). These experiments as well as the low yields obtained using $K_2S_2O_8$ alone suggest the major pathway for product formation is not light- or thermal-driven O−O bond homolysis followed by SET and is driven by the combined action of the photocatalyst and oxidant. Furthermore, no correlation was observed between the excited state triplet energies of the photocatalysts examined and starting material consumption (see the Supporting Information for details). These experiments imply that triplet energy transfer pathways are not operating in these oxidative ring-opening reactions.

Following our identification of an efficient set of conditions, we investigated the scope of the transition metal-free oxidative C−N cleavage protocol (Figure 3). Various substitution patterns on the piperidine ring were tolerated, providing access to the corresponding acyclic amines in moderate to good yields (43−95%). For example, 4-substituted piperidines
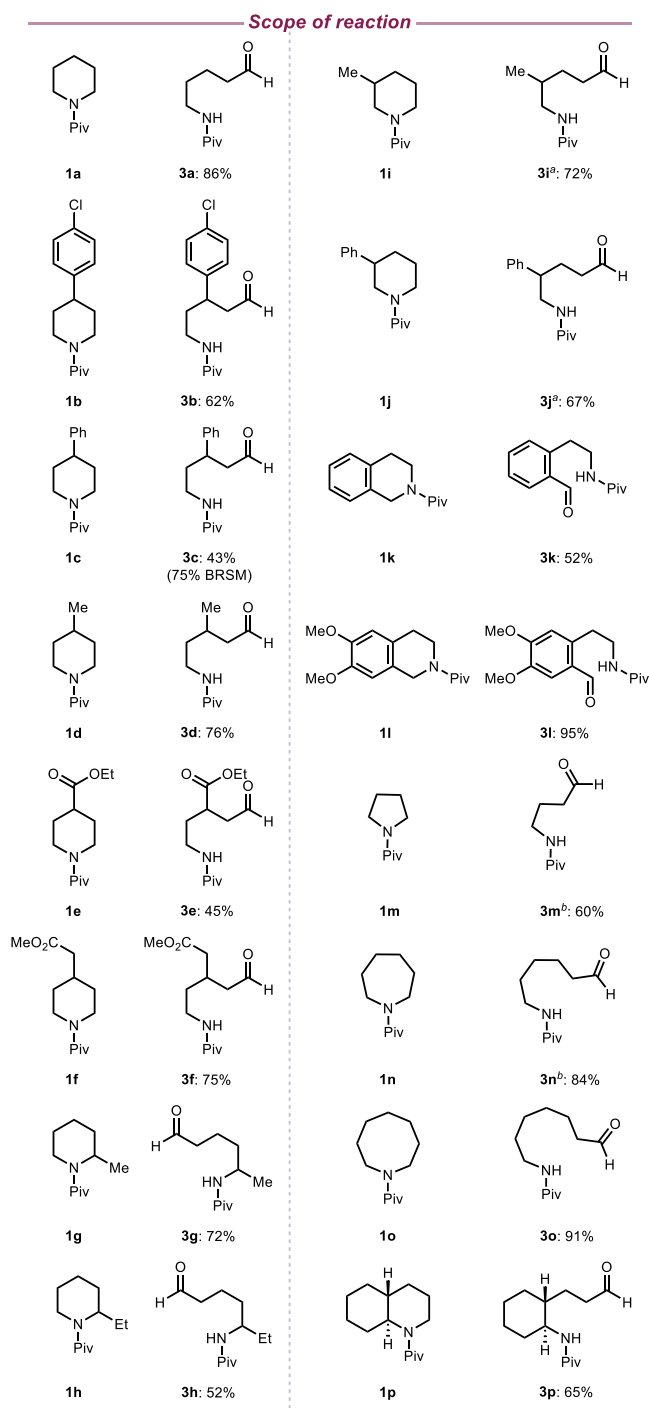
— Scope of reaction —



**Figure 3.** Cyclic amine scope. Only isolated yields are shown. Reaction conditions: cyclic amine (0.2 mmol), **2a** (5 mol %), $K_2S_2O_8$ (3 equivalents), MeCN: $H_2O$ (1:1), and 2 h. All reactions were conducted using a Kessil lamp for irradiation. [a]Major isolated constitutional isomer shown. [b]Isolated yield of acid product: **3m**: 2.5%, **3n**: 13%.

led to β-substituted aliphatic aldehydes (**3b−3f**). Notably, piperidines containing benzylic sites that are susceptible to oxidation afforded the corresponding aldehydes in 62 and 43% yield, respectively. Piperidines bearing ester functional groups on the saturated azacycle backbone (e.g., **1e** and **1f**) also worked well. Complete positional selectivity was observed when 2-substituted piperidines (**1g**, **1h**) were subjected to the

oxidative ring-opening protocol. Presumably, the selectivity that is observed is dictated by sterics in accordance with precedent.[9,10,29] However, 3-substituted piperidines (**3i**, **3j**) gave a mixture of constitutional isomers.

Our transition metal-free oxidative protocol is not limited to piperidines. For example, skeletal diversification of the tetrahydroisoquinoline skeleton, which is present in a significant number of pharmaceuticals and natural products,[31,32] is also possible. *N*-Pivaloyl-tetrahydroisoquinoline **1k** underwent oxidative ring opening to provide aldehyde **3k** in 52% yield. Notably, the C−N bond proximal to the arene ring was selectively cleaved. Furthermore, competing α-C−H abstraction was not observed despite the presence of two ether functional groups in **1l**; benzaldehyde **3l** was obtained in 95% yield. The α-arylation of ethers has been recently reported featuring open-shell alkyl radical intermediates, which add to heteroarenes (i.e., Minisci reaction).[33] In these cases, the participating radicals were generated by hydrogen atom abstraction with persulfate.

Saturated aza-cycles of various ring sizes underwent oxidative ring opening to provide the corresponding aliphatic aldehydes in moderate to good yield (60−91%). However, in the case of **3m** and **3n**, the aldehyde groups underwent subsequent oxidation to the corresponding carboxylic acids, resulting in a mixture of products that were easily separated (see the Supporting Information for details).

In order to gain insight into the transition metal-free oxidative C−N cleavage protocol, we turned to density functional theory (DFT) and time-dependent DFT calculations. Following a series of computations to validate our models (see the Supporting Information), we selected riboflavin monoacetate (**2.A.m**, where "m" stands for monoacetate) as a model for riboflavin tetraacetate (**2.A**), which was used in our experiments. The calculations show that the formation of (**2.A.m**)−[$K_2S_2O_8$] adduct is exergonic by ΔG of 5.9 kcal/mol. Since the coordination of **1a** to (**2.A.m**)−[$K_2S_2O_8$] that leads to the {(**2.A.m**)−[$K_2S_2O_8$]}−(**1a**) adduct is also exergonic (by 3.2 kcal/mol), we selected the {(**2.A.m**)−[$K_2S_2O_8$]}−(**1a**) adduct as the photon-absorbing species, which aligns with precedent demonstrating prior coordination of persulfate to the photocatalyst.[34] Here, we discuss only the energetically lowest conformers of every calculated structure and the corresponding Gibbs free energies unless otherwise stated—full computational details are described in the Supporting Information.

Our calculated reaction mechanism for the oxidation of **1a** is described in Figure 5. Irradiation of {(**2.A.m**)−[$K_2S_2O_8$]}−(**1a**) with blue light (see the Supporting Information for the computed UV−Vis spectra of {(**2.A.m**)−[$K_2S_2O_8$]}−(**1a**), (**2.A.m**)−[$K_2S_2O_8$], and **2.A.m**) leads to excitation from the $S_0$ state of {(**2.A.m**)−[$K_2S_2O_8$]}−(**1a**) to its $S_2$ bright state (see Figure 4). Its energetically lower-lying $S_1$ state is a largely dark state that is unlikely to contribute to the reaction (see the Supporting Information). The bright $S_0/S_2$ transition is the (HOMO−1)−LUMO (i.e., π−π*) transition associated with the riboflavin fragment (see the Supporting Information). The excited $S_2$ state of this system quenches to the optically dark triplet state $T_1$ (through the $T_1'$ state, see Figures 4 and 5) through the $S_0/T_1$ seam of crossing (MSX), which was determined to have a minimum point of 69.9 kcal/mol. Thus, the photoinitiated $S_0 \rightarrow T_1$ transition is controlled by the minimum on the $S_0/T_1$ seam of crossing (MSX), which is energetically easily accessible at the wavelengths used in our
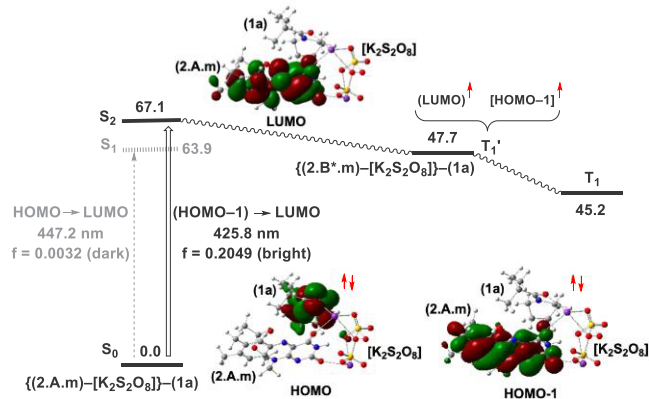
**Figure 4.** Schematic presentation of radiative generation of the $S_2$ excited state of the riboflavin-persulfate-substrate adduct $(2.A.m)-[K_2S_2O_8]-1a$. All energies are shown in kcal/mol.

experiments. The MSX serves as an interfacial "funnel", which can also be described as intersystem crossing (ISC), from the optically bright singlets to the reactive $T_1$ potential energy surface. The calculated 24.4 kcal/mol energy difference between the MSX point and the $T_1$ minimum of complex $\{(2.A.m)-[K_2S_2O_8]\}-(1a)$ is internal energy that is available to complete the HAT from cyclic amine **1a** to the excited state riboflavin-persulfate complex. This process has no associated energy barrier and forms the triplet state intermediate $\{(2.E.m)-[K_2S_2O_8]\}-(1a')$, **(T)-1**. This conclusion is consistent with parallel reaction kinetic isotope effect (KIE) studies using Piv-protected piperidine-$d_{10}$ (**1a-$d_{10}$**). The results of the parallel experiments and intermolecular competition experiments (see the Supporting Information) do not support

rate-limiting C–H bond cleavage (see Figure 6). Additionally, while we could not rule out radical chain pathways,[35] a light
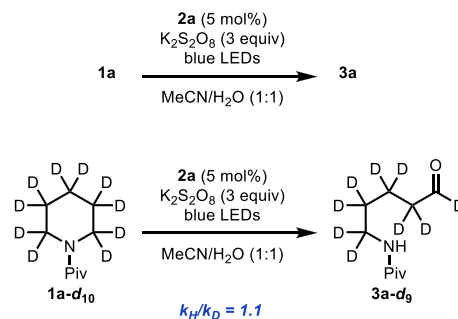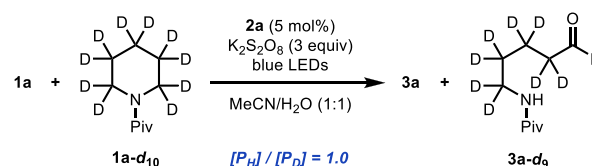


**Figure 6.** Initial rates comparison for **1a** and **1a-$d_{10}$**, $k_H/k_D = 1.1$. Intermolecular competition experiment (0.05 mmol **1a** + 0.05 mmol **1a-$d_{10}$**), $[P_H]/[P_D] = 1.0$. See the Supporting Information for full details.

on/off study revealed that any chain processes are short-lived, and irradiation is required for continued product formation (see the Supporting Information).
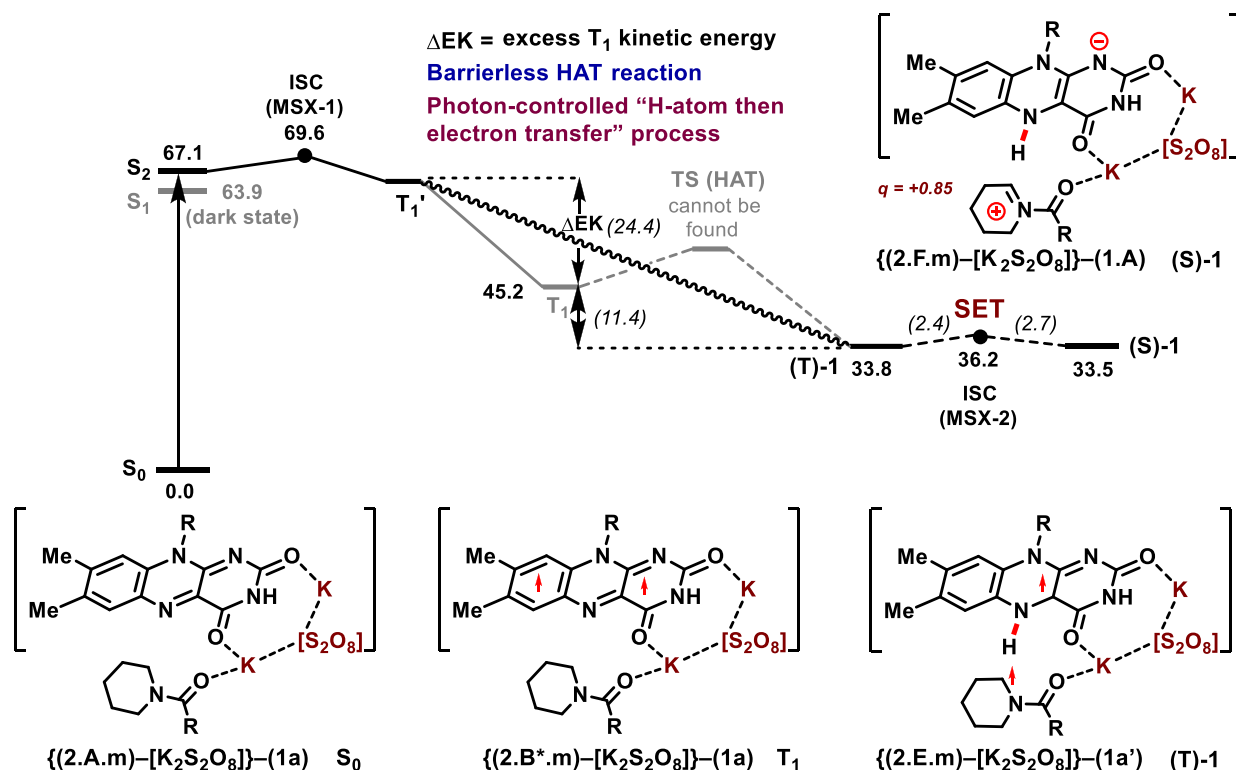


**Figure 5.** Computed reaction pathways for the oxidation of **1a** to **1.A**. All energies are Gibbs free energies listed in kcal/mol (energy differences are shown in parentheses).

Calculations show that the formation of intermediate (T)-1 is exergonic by 11.4 kcal/mol, relative to the optimized $T_1$ state. Our computational analyses show that (T)-1 possesses one less $\alpha$-amino H-atom and has almost one full $\alpha$-spin. Another unpaired $\alpha$-spin is located in the riboflavin fragment. The subsequent single-electron transfer (SET) from the $\alpha$-amino radical (i.e., 1a′) to $\{(2.E.m)-[K_2S_2O_8]\}$ in (T)-1 is almost thermoneutral. In the resulting singlet state intermediate $\{(2.F.m)-[K_2S_2O_8]\}-(1.A)$, (i.e., (S)-1), the iso-alloxazine is fully reduced and iminium ion 1.A has formed. Extensive analyses show that the (T)-1 → (S)-1 transition occurs through the triplet-to-singlet seam of crossing (MSX), which has a minimum point located only ~2.4 kcal/mol higher than (T)-1; therefore, the SET in (T)-1 is a facile process and the (T)-1, (S)-1 transition is exergonic by only 0.3 kcal/mol. Dissociation of iminium ion 1.A from (S)-1 requires only 10.4 kcal/mol and completes the formation of the iminium ion and intermediate (S)-2 (see the Supporting Information for subsequent reactions from the (S)-2 intermediate).

In summary, our calculations show that irradiation of a mixture of riboflavin tetraacetate, modeled as riboflavin monoacetate (2.A.m), potassium persulfate, and N-Piv-piperidine 1a with blue light generates the triplet state intermediate $\{(2.B*.m)-[K_2S_2O_8]\}-(1a)$ (T₁) through the $S_0/T_1$ seam of crossing (MSX), which is energetically accessible at the wavelengths used in our experiments. The iminium ion (1.A) generation from the $T_1$ intermediate is a barrierless, photon-controlled process and occurs by a stepwise "H-atom *then* electron transfer" mechanism. This conclusion is the opposite of our initial hypothesis involving "electron *then* H-atom transfer" but is consistent with our experimental KIE studies.

**Copper-Mediated Deconstructive Functionalization.** During our investigation of the photocatalytic oxidative ring opening of cyclic amines, we noted, in some cases, the subsequent oxidation of the generated aldehyde products to the corresponding carboxylic acids. Given the potential of these readily accessed carboxylic acids in subsequent derivatizations, we also explored complementary transition metal-mediated processes that would achieve oxidation of the aldehyde and provide access to alkyl carboxylic acids. Given the mild oxidation properties of copper salts (Cu(II)/Cu(I): −0.09 V vs SCE;[36] Flavins: +1.67 V vs SCE;[37] N-acyl cyclic amines: +1.13 V vs SCE[9]), we envisaged a process in which a Cu(I) salt is oxidized by persulfate to Cu(II), forming a sulfate ion and a sulfate radical anion as byproducts. Under these conditions, oxidation of cyclic amine substrates through a HAT/SET process analogous to that depicted in Scheme 1 was expected. Upon formation of the open-chain aldehyde, a second oxidation to the carboxylic acid would be achieved through a Cu(II)/Cu(I) cycle.

Following optimization of the reaction conditions (see the Supporting Information for details), N-Piv-piperidine was converted to carboxylic acid 4a in 55% yield using 25 mol % Cu(MeCN)₄BF₄ and 4 equivalents of sodium persulfate in an acetone/water mixture. Cyclic amines of various ring sizes (1m−1o, Figure 7) also underwent ring opening to form carboxylic acids with a range of chain lengths in moderate yield (53−61%). Piperidines bearing an $\alpha$-methyl substituent (1g), analogous to our observations described above using riboflavin tetraacetate (Figure 3), exhibited selective ring opening on the less substituted side of the ring, giving the corresponding product in 49% yield. Other piperidine derivatives with various
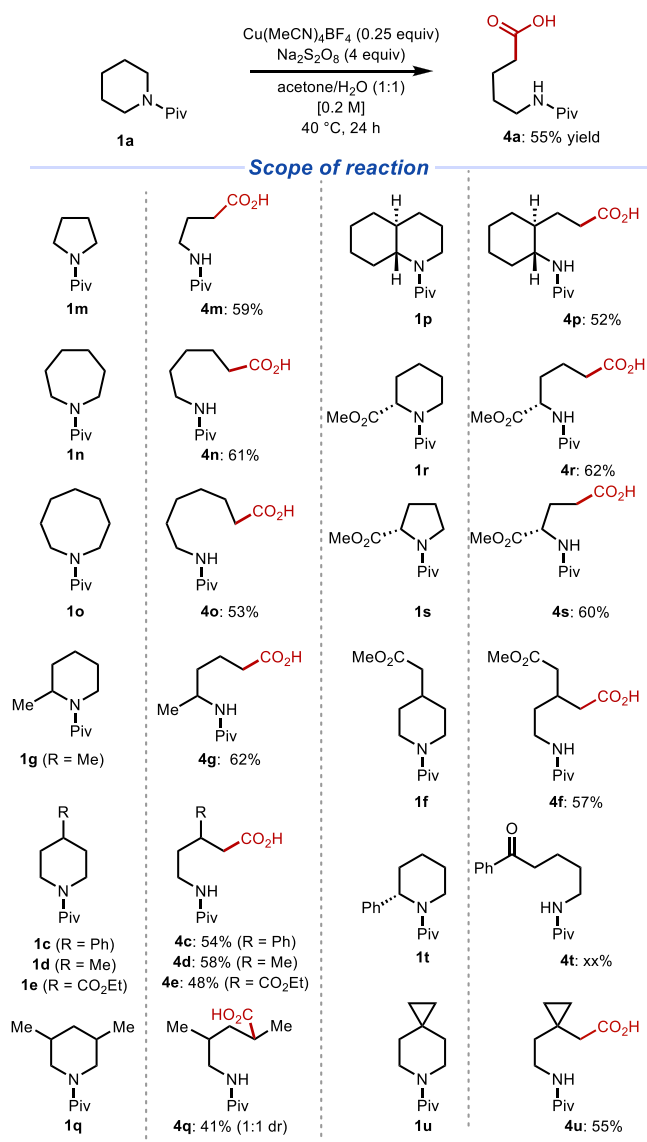


**Figure 7.** Copper-mediated oxidative ring opening of cyclic amines: reaction scope. Only isolated yields are shown. Reaction conditions: cyclic amine (0.2 mmol), Cu(MeCN)₄BF₄ (25 mol %), Na₂S₂O₈ (4 equivalents), acetone/H₂O (1:9), 24 h. [a]Reaction performed in acetone/H₂O (1:1). [b]Reaction performed with 1 equivalent of Cu(MeCN)₄BF₄.

substitution patterns (1c−1e, 1q) also participated in the ring opening. Esters and other substituents that possess activated benzylic hydrogens were tolerated and resulted in moderate yields (48−54%). The Cu(I)-mediated ring-opening reaction was also extended to other medicinally relevant saturated azacycles including perhydroquinoline (1p), pipecolic acid methyl ester (1r), and proline methyl ester (1s) in 52, 62, and 60% yield, respectively. Interestingly, a cyclic amine bearing an $\alpha$-phenyl substituent resulted in the formation of a linear aryl ketone product (4t) along with a small amount (9%; 21%, based on recovered starting material; brsm) of a $\delta$-keto acid product resulting from a second set of oxidations at the $\alpha$-position of the amine (see the Supporting Information for details). Spiro-fused cyclopropyl piperidine 1u was also converted to the corresponding carboxylic acid (4u; 55% yield) without competing opening of the cyclopropane, which may have occurred under more forcing conditions.

This mild oxidative ring-opening process can also be applied to the selective modification of amino acid sequences. Since polypeptides contain *N*-acylated cyclic amines in the form of proline residues, this method may provide a route for their modification.[38,39] The copper-mediated oxidative ring-opening of a proline residue effectively transforms it to a glutamate residue through this direct core modification method. As is well recognized, the cyclic structure of proline imparts unique structural characteristics to peptide sequences because of its dihedral angle.[40−42] As such, transforming a proline residue into a glutamate residue may not only impact the primary structure of a protein through a change in the amino acid sequence but could also have implications on larger-scale structures by influencing protein folding. While the transformation of a proline residue into glutamate has been reported previously,[12,17] the existing methods require the use of catalysts that are either expensive or not commercially available, and therefore, these reaction conditions might be difficult to translate into industrial processes. Our method makes use of a cheap, commercially available catalyst that does not require difficult-to-access ligands.

We demonstrated the potential for modification of peptide sequences by performing a ring-opening oxidation on two dipeptides, Pro-Thr **5a** and Pro-Val **5b** (Figure 8). The
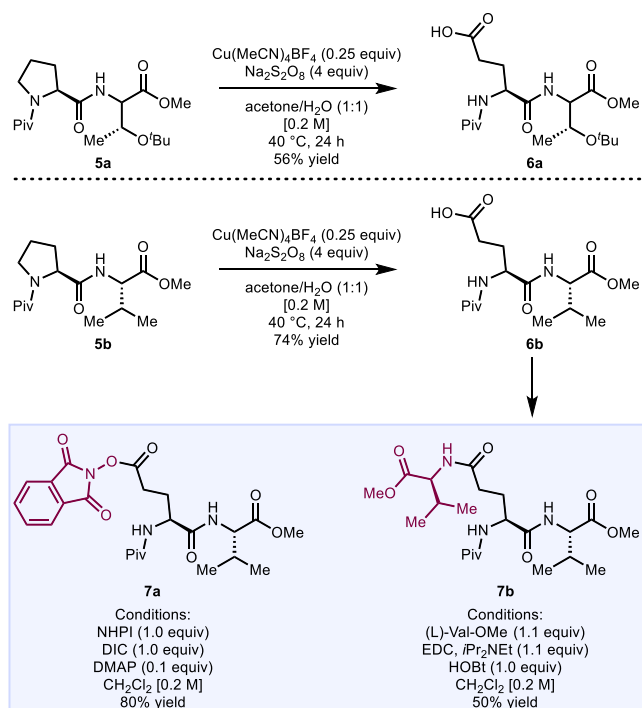


**Figure 8.** Peptide diversification. Only isolated yields are shown. See the Supporting Information for full experimental details.

resulting glutamate-bearing edited dipeptides were obtained in moderate yield (56 and 74%, respectively). Since the newly formed glutamate residue should serve as a reactive handle in esterification, amidation, and decarboxylation processes, we also briefly investigated subsequent transformations of the Glu-Val dipeptide. For example, esterification of the dipeptide with *N*-hydroxyphthalimide (NHPI) resulted in the corresponding NHPI ester (**7a**) in 80% yield. Given the emerging methods for engaging NHPI esters in cross-couplings,[43] **7a** may be used in a range of decarboxylative coupling reactions. The glutamic

acid side chain could also be engaged in simple peptide couplings. For example, an amide coupling using valine led to branched peptide **7b** in 50% yield.

## Computational Study of the Cu(I)-Mediated Deconstructive C−H Functionalization of 1a Using Sodium Persulfate (Na₂S₂O₈) as an Oxidant.

In order to gain further insight into the Cu(I)-mediated oxidative opening of aliphatic amines derivatives (e.g., **1a**) to form ring-opened carboxylic acids, we launched DFT studies using CuBF₄ to model Cu(I), *N*-Piv-piperidine **1a** as a substrate, and sodium persulfate (Na₂S₂O₈) as an oxidant (see the Supporting Information for details). Similar to our previously reported Ag(I)-mediated C−C deconstructive fluorination of *N*-benzoylated cyclic amines using Selectfluor,[9,44] one would expect either **1a** (represented as **LH** in Figure 9 to highlight
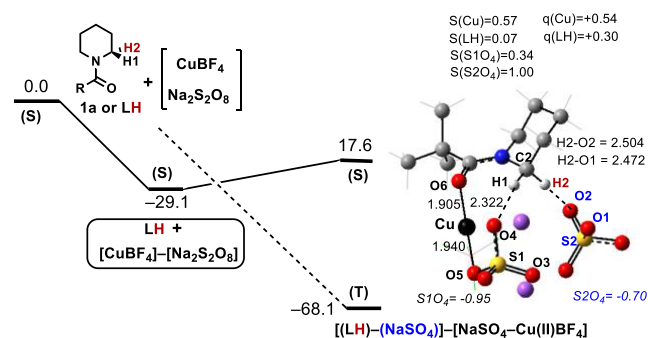


**Figure 9.** Computed reaction mechanism for the formation of intermediate [(**LH**)−(NaSO₄)]−[NaSO₄−Cu(II)BF₄] upon reaction of CuBF₄, **LH**, and sodium persulfate (Na₂S₂O₈). Here, Gibbs free energies are in kcal/mol. Labels (S) and (T) represent the singlet and triplet electronic states, respectively. Spin densities, S(X), and Mulliken charges, q(X), are given in |e|. Geometries are in Å. BF₄ anions are omitted for clarity.

and closely follow the anticipated H-atom transfer) or sodium persulfate coordination to the Cu(I)-center as a first step. Our calculations show that sodium persulfate coordination to CuBF₄ is thermodynamically more favorable by 2.9 kcal/mol (26.2 vs 29.1 kcal/mol for the direct H-atom transfer) and leads to the singlet state adduct [CuBF₄]−[Na₂S₂O₈] (see the Supporting Information for more details).

From singlet state adduct [CuBF₄]−[Na₂S₂O₈], SET could occur either prior to or after substrate coordination to the Cu(I)-center. In either case, SET from the Cu(I) center to sodium persulfate leads to the O−O bond cleavage and formation of sodium sulfate and a sulfate radical anion. Should the SET occur prior to substrate coordination to the Cu(I) center, the ring-opened aldehyde product (**3a** in Scheme 1) will form through a radical pathway initiated by H-atom abstraction by the sulfate radical anion (as shown in Scheme 1). However, our calculations show that the SET most likely occurs upon substrate coordination to the Cu(I) center since the formation of the triplet state Cu(II) intermediate [(**LH**)−(NaSO₄)]−[NaSO₄−Cu(II)BF₄] is highly favored relative to the dissociation limit of (**LH**) + [CuBF₄]−[Na₂S₂O₈]. Interestingly, as can be seen in Figure 9, in the Cu(II) intermediate [(**LH**)−(NaSO₄)]−[NaSO₄−Cu(II)BF₄], the S1O₄ sulfate anion (left side of the structure, each SO₄ unit here is denoted as S1O₄ or S2O₄ for distinction) is coordinated to the Cu(II)-center (Cu−O5 bond length = 1.940 Å). The second sulfate anion (S2O₄) is weakly associated with the Cu-
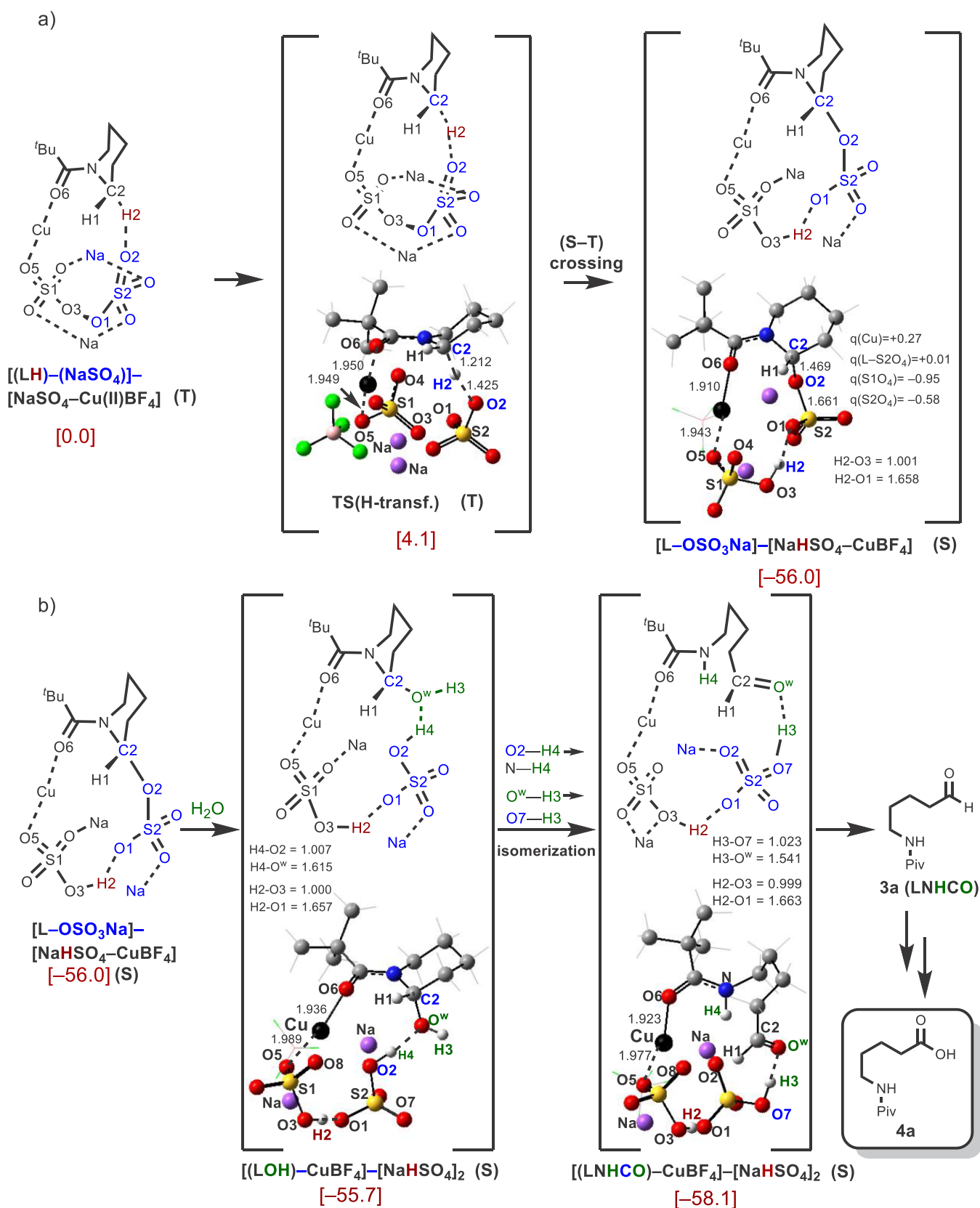
a)



b)



**Figure 10.** Computed ring-opening mechanism in intermediate $[(\textbf{LH})-(NaSO_4)]-[NaSO_4-Cu(II)BF_4]$. Gibbs free energies are reported in kcal/mol. Label (S) represents a singlet electronic state. Bond lengths are reported in Å. For simplicity, the $BF_4$ fragment is omitted.

coordinated substrate (H2−O2 = 2.504 Å and H2−O1 = 2.472 Å). These sulfate anions are bridged by the two sodium cations. Since the SET is expected to be very fast and occur

through the singlet-to-triplet seam of crossing for the $[CuBF_4]-[Na_2S_2O_8]$ complex, it should not impact the rate of reaction or reaction outcome. Therefore, here, an in-depth

analysis of this path was not conducted.[45,46] The next step of the reaction, H-atom abstraction from the C2-position of the *N*-acylated piperidine substrate by the $S_2O_4$ sulfate anion, is illustrated in Figure 10a. This step is a two-state reactivity event (i.e., starts from a triplet state prereaction complex and results in a singlet state product) that has a small free energy barrier of 4.1 kcal/mol at the triplet state transition state **TS(H-transf.)**. The net process is highly exergonic (by 56.0 kcal/mol). Interestingly, intrinsic reaction coordinate (IRC) calculations show that while this process begins with abstraction of a H-atom from C2 by the O2-atom of the $S_2O_4$ sulfate anion at **TS(H-transf.)**, it culminates in a product where the abstracted H-atom has been transferred to the second sulfate anion (i.e., $S_1O_4$) and the O2-atom of the $S_2O_4$ sulfate anion is coordinated to the piperidine ring at the C2-position. Overall, this H-atom abstraction event leads to the formation of a singlet state product $[L\text{-}OSO_3Na]\text{-}[NaHSO_4\text{-}CuBF_4]$, which is a complex of the $[L\text{-}OSO_3Na]$ and $[NaHSO_4\text{-}CuBF_4]$ fragments. Charge density analyses show that the $[L\text{-}OSO_3Na]$ unit possesses an overall +0.57 |e| charge.

Calculations show that in the presence of water molecules (see Figure 10b), intermediate $[L\text{-}OSO_3Na]\text{-}[NaHSO_4\text{-}CuBF_4]$ is in equilibrium with the hemiaminal (i.e., $[(LOH)\text{-}CuBF_4]\text{-}[NaHSO_4]_2$). The hemiaminal is the product of $H\text{-}O^wH$ hydrolysis of the $L\text{-}OSO_3Na$ bond. Multiple proton-shuttles occur between the N-center of the substrate and $HSO_4^-$ unit, as well as between the LOH and $HSO_4^-$ units, which leads to formation of intermediate $[(\textbf{LNHCO})\text{-}CuBF_4]\text{-}[NaHSO_4]_2$. Calculations show that $[(\textbf{LNHCO})\text{-}CuBF_4]\text{-}[NaHSO_4]_2$ is only 2.4 kcal/mol lower in free energy than the $[(LOH)\text{-}CuBF_4]\text{-}[NaHSO_4]_2$ complex. At this time, we cannot rule out the formation of $[(\textbf{LNHCO})\text{-}CuBF_4]\text{-}[NaHSO_4]_2$ through outer-sphere protonation—deprotonation by other molecules of water from the solvent.

Dissociation of **LNHCO** from $[(\textbf{LNHCO})\text{-}CuBF_4]\text{-}[NaHSO_4]_2$ leads to the final product. The computational data presented above shows that the overall reaction (**LH**) + $CuBF_4$ + $Na_2S_2O_8 \rightarrow (\textbf{LNHCO})$ + $[CuBF_4]\text{-}[NaHSO_4]_2$ is highly exergonic (by 126.2 kcal/mol) and will proceed spontaneously without a significant energy barrier. Under the oxidative reaction conditions, it is likely that the resulting aldehyde (**3a**) is oxidized to the corresponding carboxylic acid **4a** (see Figure 10B).[47]

**Ring-Opening Minisci Reaction.** With access to various carboxylic acid derivatives through our oxidative ring-opening process, we envisioned engaging them in one-pot coupling reactions. To this end, we turned toward $Csp^3\text{-}Csp^2$ bond formation using a radical decarboxylation process and addition of the resulting alkyl radical to a heterocycle acceptor. We have previously demonstrated access to a proposed primary alkyl radical through a series of oxidations with a Ag(I) salt and persulfate oxidant.[10] Therefore, we hypothesized that this radical might engage a coupling partner in carbon—carbon bond forming processes. This type of $Csp^3\text{-}Csp^2$ bond formation has recently been demonstrated in radical additions to quinones through a silver-mediated deconstructive process,[29] as well as an analogous Minisci process.[30] Since the conditions for the deconstructive process that lead to an alkyl radical are somewhat acidic (as a result of the formation of hydrogen sulfate ions and carbonic acid), we hypothesized that these conditions would be amenable to Minisci-type

reactions,[20] which proceed more favorably upon protonation of a heteroarene acceptor.

Following optimization of the reaction conditions, treatment of Piv-protected piperidine **1a** with the Ag(I)/persulfate conditions and 4-trifluoromethylpyridine under acidic conditions (trifluoroacetic acid) afforded the corresponding amino-alkyl substituted pyridine in 50% yield (Figure 11).
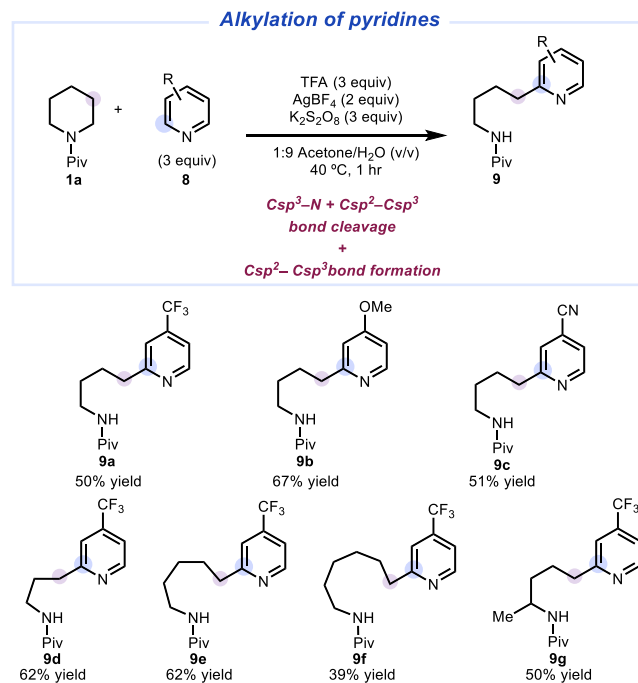


**Figure 11.** Deconstructive Minisci reaction scope. Only isolated yields are shown. See the Supporting Information for full experimental details.

Pyridines bearing electron donating/withdrawing substituents were also competent in this coupling reaction, forming the desired products (**9a–9c**) in moderate yet useful yields (50–67%). We next subjected cyclic amines of various ring sizes (**9d–9f**) to the same conditions, again providing the alkylation products in moderate yield (39–62%). A 2-methyl substituted piperidine derivative also underwent the expected ring-opening selectively away from the substituted side of the ring (**9g**).

**Autocyclization Using Cu(II) Oxidation.** Finally, we also investigated the interception of the proposed alkyl radical intermediate with other transition metals. Particularly, since De La Mare and coworkers[48,49] previously reported the formation of alkenes from alkyl radicals through an oxidation by Cu(II) followed by an elimination, we wondered whether we could gain access to terminal olefins from the primary radical generated through the deconstructive process. However, upon the addition of a Cu(II) source to the Ag(I)/persulfate reagents for the deconstructive functionalization of Piv-protected pyrrolidine, we did not detect any of the expected alkene product. Instead, we observed the formation of an oxazine in 85% yield (Figure 12). This heterocycle may arise from oxidation of the alkyl radical by Cu(II) and intramolecular nucleophilic trapping by the amide carbonyl oxygen instead of elimination to generate an olefin. The structure of **10m** was unambiguously confirmed by X-ray crystallography. The formation of these oxazine heterocycles has previously been reported from the autocyclization of γ-bromo alkyl
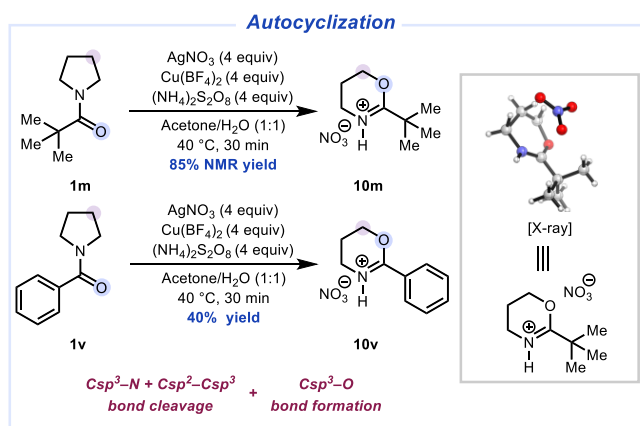
**Figure 12.** Autocyclization of cyclic amines. Isolated yields are shown unless otherwise noted. See the Supporting Information for full experimental details and crystallographic data.

amides.[50] We extended the transformation to the ring opening and subsequent cyclization of *N*-Bz-pyrrolidine (**1v**) to provide phenyl-substituted oxazine **10v** in 40% yield. The transformation of pyrrolidines to oxazines represents an effective strategy to access new chemical space in medicinal chemistry.

Since the formation of the oxazines did not align with our initial hypothesis, we embarked upon an examination of the mechanism for their formation using DFT calculations, as summarized in Figure 13. We have previously investigated a
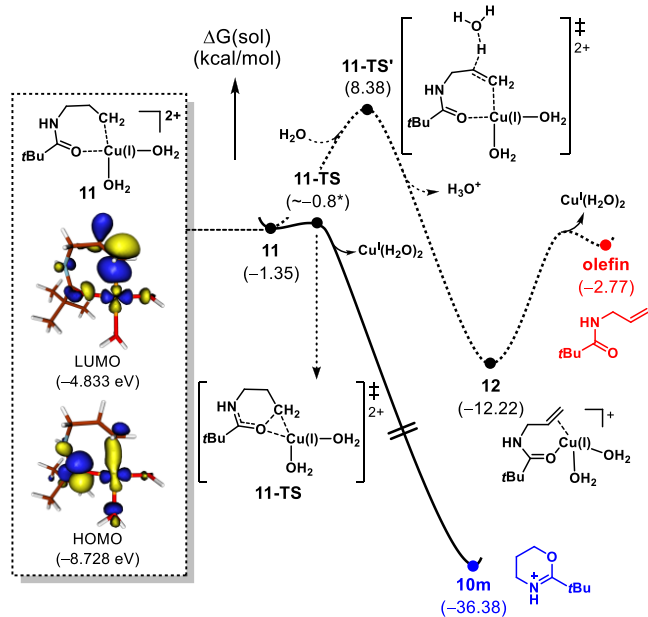


**Figure 13.** Free energy profile for the oxazine formation by Cu(II). See the Supporting Information for full computational details.

mechanism for the generation of an alkyl radical from a cyclic amine using Ag(I) and persulfate.[10,44] Here, we propose that the alkyl radical is similarly formed prior to interacting with Cu(II) to form complex **11**, although the exact details continue to be investigated. While the combination of a carbon-centered radical with Cu(II) is often depicted as a Cu(III) intermediate,[51,52] we recognize that these types of copper complexes may have an electronic structure that reflects a Cu(I) center, in which a formal reduction of Cu(II) occurs.[53]

Our calculations suggest that deprotonation to form the alkene has an associated barrier of 9.7 kcal/mol, while the competing intramolecular cyclization is essentially barrierless. Even though **11** is hydrated and the concentration of $H_2O$ is ~500 times higher than the copper complex, calculations suggest that the intrinsic reaction rate of cyclization should be about $5 \times 10^6$ times faster than deprotonation (see the Supporting Information for details). Therefore, the cyclization should be the dominant pathway. Indeed, a screen of various copper salts, which would otherwise lead to products such as olefination and halogenation of primary alkyl radicals,[49] revealed that only the linear aldehyde **3m**, carboxylic acid **4m**, and cyclization product **10m** could be obtained (see the Supporting Information for details). The rapid cyclization can also be rationalized on the basis of the frontier molecular orbitals of **11**. While the orbitals of **11** are all interacting, there is a prominent interaction between the HOMO and LUMO orbitals that informs the observed cyclization to oxepine **10m**. As shown in Figure 13, the shape of the nucleophilic HOMO on the amidyl oxygen and the low energy LUMO on the primary alkyl in **11** are reasonably well matched for the favorable intramolecular HOMO−LUMO interaction.[54]

## ■ CONCLUSIONS

In summary, we have developed a range of deconstructive functionalizations of cyclic aliphatic amines to achieve skeletal diversification that builds on our previous reports.[9−11] We developed two methods for ring-opening transformations, achieving an organo-photocatalytic formation of linear aldehydes with riboflavin tetraacetate and a Cu(I)-mediated oxidation to access amine derivatives bearing carboxylic acid groups. We have also reported a combined organo-photo-catalytic/transition metal-mediated oxidative ring-opening procedure for high-yielding formation of carboxylic acids (see the Supporting Information). Our calculations of the photoinduced oxidation of piperidines by riboflavin tetraace-tate suggest that the oxidation is initiated by a photon-driven HAT.

We have also developed a ring-opening C−C bond formation process that takes advantage of a decarboxylative $Csp^3$−$Csp^2$ Minisci coupling reaction. While our lab previously reported the formation of alkyl halides through a similar transformation that could serve as precursors for C−C bond formation,[10] the Minisci process reported here provides direct access to value-added C−C coupled products. A second study aimed at a one-pot, multimetallic, decarboxylative trans-formation led to the formation of oxazines. Additional investigations to expand the scope of oxazine formation from cyclic amines are ongoing in our lab.

In the studies presented here, persulfate emerged as a versatile oxidant that could be tuned by pairing it with various transition metals and organic photocatalysts to selectively oxidize various substrates. The multiple means by which the peroxy bond can be homolyzed, in combination with the oxidation potential and H-atom abstraction ability of the sulfate radical anion, allow for many different oxidative processes. The versatility of cyclic amines as substrates for late-stage diversification as reported here rests on their ability to serve as latent alkyl radicals. These studies, as well as previous reports from our laboratories and others, demonstrate high potential for skeletal modification of cyclic amines by the generation of an alkyl radical through oxidative ring opening.

Other pathways for structural diversification of cyclic aliphatic amines are currently under investigation in our lab.

## ASSOCIATED CONTENT

### Supporting Information

The Supporting Information is available free of charge at https://pubs.acs.org/doi/10.1021/jacs.3c01318.

Experimental procedures, computational details, and compound characterization (PDF)

### Accession Codes

CCDC 2128702 contains the supplementary crystallographic data for this paper. These data can be obtained free of charge via www.ccdc.cam.ac.uk/data_request/cif, or by emailing data_request@ccdc.cam.ac.uk, or by contacting The Cambridge Crystallographic Data Centre, 12 Union Road, Cambridge CB2 1EZ, UK; fax: +44 1223 336033.

## AUTHOR INFORMATION

### Corresponding Authors

**Mu-Hyun Baik** − *Department of Chemistry, Korea Advanced Institute of Science and Technology (KAIST), Daejeon 34141, Korea; Center for Catalytic Hydrocarbon Functionalizations, Institute for Basic Science (IBS), Daejeon 34141, Korea;* orcid.org/0000-0002-8832-8187; Email: mbaik2805@kaist.ac.kr

**Djamaladdin G. Musaev** − *Cherry L. Emerson Center for Scientific Computation, and Department of Chemistry, Emory University, Atlanta, Georgia 30322, United States;* orcid.org/0000-0003-1160-6131; Email: dmusaev@emory.edu

**Richmond Sarpong** − *Department of Chemistry, University of California, Berkeley, California 94720, United States;* orcid.org/0000-0002-0028-6323; Email: rsarpong@berkeley.edu

### Authors

**David M. Soro** − *Department of Chemistry, University of California, Berkeley, California 94720, United States*

**Jose B. Roque** − *Department of Chemistry, University of California, Berkeley, California 94720, United States; Present Address: Department of Chemistry, Princeton University, Princeton, New Jersey 08544, United States (J.B.R.);* orcid.org/0000-0002-5449-1584

**Jonas W. Rackl** − *Department of Chemistry, University of California, Berkeley, California 94720, United States; Present Address: Laboratory of Organic Chemistry, ETH Zurich, Zurich, Switzerland (J.W.R.).*

**Bohyun Park** − *Department of Chemistry, Korea Advanced Institute of Science and Technology (KAIST), Daejeon 34141, Korea; Center for Catalytic Hydrocarbon Functionalizations, Institute for Basic Science (IBS), Daejeon 34141, Korea;* orcid.org/0000-0003-0552-8763

**Stefan Payer** − *Department of Chemistry, University of California, Berkeley, California 94720, United States; Present Address: Institute of Chemistry, University of Graz, Graz, Austria (S.E.P)*

**Yuan Shi** − *Discovery Chemistry Research and Technologies, Eli Lilly and Company, Indianapolis, Indiana 46285, United States*

**J. Craig Ruble** − *Discovery Chemistry Research and Technologies, Eli Lilly and Company, Indianapolis, Indiana 46285, United States*

**Alexey L. Kaledin** − *Cherry L. Emerson Center for Scientific Computation, and Department of Chemistry, Emory University, Atlanta, Georgia 30322, United States;* orcid.org/0000-0003-3112-3989

Complete contact information is available at:
https://pubs.acs.org/10.1021/jacs.3c01318

## REFERENCES

(1) Blakemore, D. C.; Castro, L.; Churcher, I.; Rees, D. C.; Thomas, A. W.; Wilson, D. M.; Wood, A. Organic synthesis provides opportunities to transform drug discovery. *Nat. Chem.* **2018**, *10*, 383−394.

(2) Cernak, T.; Dykstra, K. D.; Tyagarajan, S.; Vachal, P.; Krska, S. W. The medicinal chemist's toolbox for late stage functionalization of drug-like molecules. *Chem. Soc. Rev.* **2016**, *45*, 546−576.

(3) Corey, E. J.; Howe, W. J.; Orf, H. W.; Pensak, D. A.; Petersson, G. General methods of synthetic analysis. Strategic bond disconnections for bridged polycyclic structures. *J. Am. Chem. Soc.* **1975**, *97*, 6116−6124.

(4) Hoffmann, R. W. *Elements of Synthesis Planning*; Springer, 2009.

(5) Huigens, R. W., III; Morrison, K. C.; Hicklin, R. W.; Flood, T. A., Jr.; Richter, M. F.; Hergenrother, P. J. A ring-distortion strategy to construct stereochemically complex and structurally diverse compounds from natural products. *Nat. Chem.* **2013**, *5*, 195−202.

(6) Hu, Y.; Stumpfe, D.; Bajorath, J. Recent advances in scaffold hopping. *J. Med. Chem.* **2017**, *60*, 1238−1246.

(7) Vitaku, E.; Smith, D. T.; Njardarson, J. T. Analysis of the structural diversity, substitution patterns, and frequency of nitrogen heterocycles among U.S. FDA approved pharmaceuticals. *J. Med. Chem.* **2014**, *57*, 10257−10274.

(8) Lamberth, C. Heterocyclic Chemistry in Crop Protection. *Pest Manage. Sci.* **2013**, *69*, 1106−1114.

(9) Roque, J. B.; Kuroda, Y.; Göttemann, L. T.; Sarpong, R. Deconstructive fluorination of cyclic amines by carbon-carbon cleavage. *Science* **2018**, *361*, 171−174.

(10) Roque, J. B.; Kuroda, Y.; Göttemann, L. T.; Sarpong, R. Deconstructive diversification of cyclic amines. *Nature* **2018**, *564*, 244−248.

(11) Jurczyk, J.; Lux, M. C.; Adpressa, D.; Kim, S. F.; Lam, Y.; Yeung, C. S.; Sarpong, R. Photo-mediated ring contraction of saturated heterocycles. *Science* **2021**, *373*, 1004−1012.

(12) Onomura, O.; Moriyama, A.; Fukae, K.; Yamamoto, Y.; Maki, T.; Matsumura, Y.; Demizu, Y. Oxidative C−C bond cleavage of N-alkoxycarbonylated cyclic amines by sodium nitrite in trifluoroacetic acid. *Tetrahedron Lett.* **2008**, *49*, 6728−6731.

(13) Yamamoto, K.; Toguchi, H.; Harada, T.; Kuriyama, M.; Onomura, O. Oxidative C−C Bond Cleavage of N-Protected Cyclic Amines by $HNO_3$-TFA System. *Heterocycles* **2020**, *101*, 486−495.

(14) He, K.; Zhang, T.; Zhang, S.; Sun, Z.; Zhang, Y.; Yuan, Y.; Jia, X. Tunable Functionalization of Saturated C−C and C−H Bonds of *N,N′*-Diarylpiperazines Enabled by *tert*-Butyl Nitrite (TBN) and $NaNO_2$ Systems. *Org. Lett.* **2019**, *21*, 5030−5034.

(15) Ito, R.; Umezawa, N.; Higuchi, T. Unique Oxidation Reaction of Amides with Pyridine-N-Oxide Catalyzed by Ruthenium Porphyrin: Direct Oxidative Conversion of N-Acyl-l-Proline to N-Acyl-l-Glutamate. *J. Am. Chem. Soc.* **2004**, *127*, 834−835.

(16) Kaname, M.; Yoshifuji, S.; Sashida, H. Ruthenium tetroxide oxidation of cyclic N-acylamines by a single layer method: formation of ω-amino acids. *Tetrahedron Lett.* **2008**, *49*, 2786−2788.

(17) Osberger, T. J.; Rogness, D. C.; Kohrt, J. T.; Stepan, A. F.; White, M. C. Oxidative Diversification of Amino Acids and Peptides by Small-Molecule Iron Catalysis. *Nature* **2016**, *537*, 214−219.

(18) Sperry, J. The Oxidation of Amides to Imides: A Powerful Synthetic Transformation. *Synthesis* **2011**, 3569−3580.

(19) Latimer, W. M. *The oxidation states of the elements and their potentials in aqueous solutions*; Prentice-Hall, 1939.

(20) Minisci, F.; Citterio, A.; Giordano, C. Electron-transfer processes: peroxydisulfate, a useful and versatile reagent in organic synthesis. *Acc. Chem. Res.* **1983**, *16*, 27−32.

(21) Mandal, S.; Bera, T.; Dubey, G.; Saha, J.; Laha, J. K. Uses of $K_2S_2O_8$ in metal-catalyzed and metal-free oxidative transformations. *ACS Catal.* **2018**, *8*, 5085−5144.

(22) Batista, V. F.; Galman, J. L.; Pinto, D. C. G. A.; Silva, A. M. S.; Turner, N. J. Monoamine Oxidase: Tunable Activity for Amine Resolution and Functionalization. *ACS Catal.* **2018**, *8*, 11889−11907.

(23) Cibulka, R.; Fraaije, M. W., Eds. *Flavin-Based Catalysis: Principles and Applications*; Wiley-VCH, 2021.

(24) Lee, J.; von Gunten, U.; Kim, J.-H. Persulfate-Based Advanced Oxidation: Critical Assessment of Opportunities and Roadblocks. *Environ. Sci. Technol.* **2020**, *54*, 3064−3081.

(25) Metzler, D. E.; Cairns, W. L. Photochemical Degradation of Flavines. VI. New Photoproduct and Its Use in Studying the Photolytic Mechanism. *J. Am. Chem. Soc.* **1971**, *93*, 2772−2777.

(26) Kino, K.; Kobayashi, T.; Arima, E.; Komori, R.; Kobayashi, T.; Miyazawa, H. Photoirradiation Products of Flavin Derivatives, and the Effects of Photooxidation on Guanine. *Bioorg. Med. Chem. Lett.* **2009**, *19*, 2070−2074.

(27) Smith, E. C.; Metzler, D. E. The Photochemical Degradation of Riboflavin. *J. Am. Chem. Soc.* **1963**, *85*, 3285−3288.

(28) Crist, R. H. The Quantum Efficiency of the Photochemical Decomposition of Potassium Persulfate. *J. Am. Chem. Soc.* **1932**, *54*, 3939−3942.

(29) Liu, R.-H.; He, Y.-H.; Yu, W.; Zhou, B.; Han, B. Silver-Catalyzed Site-Selective Ring-Opening and C−C Bond Functionalization of Cyclic Amines: Access to Distal Aminoalkyl-Substituted Quinones. *Org. Lett.* **2019**, *21*, 4590−4594.

(30) Hong, S.; Kweon, B.; Lee, W.; Chang, S.; Hong, S. Deconstructive Pyridylation of Unstrained Cyclic Amines through a One-Pot Umpolung Approach. *Org. Lett.* **2023**, *25*, 2722−2727.

(31) Faheem; Kumar, B. K.; Sekhar, K. V. G. C.; Chander, S.; Kunjiappan, S.; Murugesan, S. Medicinal Chemistry Perspectives of 1,2,3,4-Tetrahydroisoquinoline Analogs − Biological Activities and SAR Studies. *RSC Adv.* **2021**, *11*, 12254−12287.

(32) Faheem; Kumar, B. K.; Sekhar, K. V. G. C.; Chander, S.; Kunjiappan, S.; Murugesan, S. 1,2,3,4-Tetrahydroisoquinoline (THIQ) as Privileged Scaffold for Anticancer de Novo Drug Design. *Expert Opin. Drug Discovery* **2021**, *16*, 1119−1147.

(33) Jin, J.; MacMillan, D. W. C. Direct α-Arylation of Ethers through the Combination of Photoredox-Mediated C−H Functionalization and the Minisci Reaction. *Angew. Chem., Int. Ed.* **2015**, *54*, 1565−1569.

(34) Kaledin, A. L.; Huang, Z.; Geletii, Y. V.; Lian, T.; Hill, C. L.; Musaev, D. G. Insights into Photoinduced Electron Transfer between $[Ru(bpy)_3]_2^+$ and $[S_2O_8]^{2−}$ in Water: Computational and Experimental Studies. *J. Phys. Chem. A* **2009**, *114*, 73−80.

(35) Cismesia, M. A.; Yoon, T. P. Characterizing chain processes in visible light photoredox catalysis. *Chem. Sci.* **2015**, *6*, 5426−5434.

(36) *Handbook of Chemistry and Physics 103rd Edition.* https://hbcp. chemnetbase.com/faces/contents/ContentsSearch.xhtml (accessed October 18, 2021).

(37) Mühldorf, B.; Wolf, R. Photocatalytic Benzylic C−H Bond Oxidation with a Flavin Scandium Complex. *Chem. Commun.* **2015**, *51*, 8425−8428.

(38) Maza, J. C.; Ramsey, A. V.; Mehare, M.; Krska, S. W.; Parish, C. A.; Francis, M. B. Secondary Modification of Oxidatively-Modified Proline N-Termini for the Construction of Complex Bioconjugates. *Org. Biomol. Chem.* **2020**, *18*, 1881−1885.

(39) Hoyt, E. A.; Oliveira, B. L.; Bernardes, G. J. L. Contemporary approaches to site-selective protein modification. *Nat. Rev. Chem.* **2019**, *3*, 147−171.

(40) Li, S. C.; Goto, N. K.; Williams, K. A.; Deber, C. M. Alpha-Helical, but Not Beta-Sheet, Propensity of Proline Is Determined by Peptide Environment. *Proc. Natl. Acad. Sci. U. S. A.* **1996**, *93*, 6676−6681.

(41) Jacob, J.; Duclohier, H.; Cafiso, D. S. The Role of Proline and Glycine in Determining the Backbone Flexibility of a Channel-Forming Peptide. *Biophys. J.* **1999**, *76*, 1367−1376.

(42) Morgan, A. A.; Rubenstein, E. Proline: The Distribution, Frequency, Positioning, and Common Functional Roles of Proline and Polyproline Sequences in the Human Proteome. *PLoS One* **2013**, *8*, No. e53785.

(43) Murarka, S. N-(Acyloxy)phthalimides as Redox-Active Esters in Cross-Coupling Reactions. *Adv. Synth. Catal.* **2018**, *360*, 1735−1753.

(44) Roque, J. B.; Sarpong, R.; Musaev, D. G. Key Mechanistic Features of the Silver(I)-Mediated Deconstructive Fluorination of Cyclic Amines: Multistate Reactivity versus Single-Electron Transfer. *J. Am. Chem. Soc.* **2021**, *143*, 3889−3900.

(45) Kaledin, A. L.; Roque, J. B.; Sarpong, R.; Musaev, D. G. Computational Study of Key Mechanistic Details for a Proposed Copper (I)-Mediated Deconstructive Fluorination of N-Protected Cyclic Amines. *Top. Catal.* **2022**, *65*, 418−432.

(46) Pitts, C. R.; Bloom, S.; Woltornist, R.; Auvenshine, D. J.; Ryzhkov, L. R.; Siegler, M. A.; Lectka, T. Direct, Catalytic Monofluorination of $sp^3$ C−H Bonds: A Radical-Based Mechanism with Ionic Selectivity. *J. Am. Chem. Soc.* **2014**, *136*, 9780−9791.

(47) Subbaraman, L. R.; Santappa, M. Oxidation Studies by Peroxydisulfate. *Z. Phys. Chem.* **1966**, *48*, 172−178.

(48) De La Mare, H. E.; Kochi, J. K.; Rust, F. F. The Oxidation and Reduction of Free Radicals by Metal Salts. *J. Am. Chem. Soc.* **1963**, *85*, 1437−1449.

(49) Kochi, J. K. Mechanisms of Organic Oxidation and Reduction by Metal Complexes: Electron and Ligand transfer processes form the basis for redox reactions of radicals and metal species. *Science* **1967**, *155*, 415−424.

(50) Reddy, D. N.; Prabhakaran, E. N. Synthesis and Isolation of 5,6-Dihydro-4H-1,3-Oxazine Hydrobromides by Autocyclization of N-(3-Bromopropyl)Amides. *J. Org. Chem.* **2010**, *76*, 680−683.

(51) Gu, Q.-S.; Li, Z.-L.; Liu, X.-Y. Copper(I)-Catalyzed Asymmetric Reactions Involving Radicals. *Acc. Chem. Res.* **2019**, *53*, 170−181.

(52) Li, Z.-L.; Fang, G.-C.; Gu, Q.-S.; Liu, X.-Y. Recent Advances in Copper-Catalysed Radical-Involved Asymmetric 1,2-Difunctionalization of Alkenes. *Chem. Soc. Rev.* **2020**, *49*, 32−48.

(53) DiMucci, I. M.; Lukens, J. T.; Chatterjee, S.; Carsch, K. M.; Titus, C. J.; Lee, S. J.; Nordlund, D.; Betley, T. A.; MacMillan, S. N.; Lancaster, K. M. The Myth of $d^8$ Copper(III). *J. Am. Chem. Soc.* **2019**, *141*, 18508−18520.

(54) Zhuo, L.-G.; Liao, W.; Yu, Z.-X. A Frontier Molecular Orbital Theory Approach to Understanding the Mayr Equation and to Quantifying Nucleophilicity and Electrophilicity by Using HOMO and LUMO Energies. *Asian J. Org. Chem.* **2012**, *1*, 336−345.